Experimental demonstration of microring quadrature phase-shift keying modulators

Po Dong,[1,*] Chongjin Xie,[1] Long Chen,[1] Nicolas K. Fontaine,[1] and Young-kai Chen[2]

[1]*Bell Labs, Alcatel-Lucent, 791 Holmdel Road, Holmdel, New Jersey 07733, USA*

[2]*Bell Labs, Alcatel-Lucent, 600 Mountain Avenue, Murry Hill, New Jersey 07974, USA*

**Corresponding author: po.dong@alcatel-lucent.com*

Received January 6, 2012; revised February 4, 2012; accepted February 6, 2012;
posted February 6, 2012 (Doc. ID 161049); published March 23, 2012

Advanced optical modulation formats are a key technology to increase the capacity of optical communication networks. Mach–Zehnder modulators are typically used to generate various modulation formats. Here, we report the first experimental demonstration of quadrature phase-shift keying (QPSK) modulation using compact microring modulators. Generation of 20 Gb/s QPSK signals is demonstrated with 30 μm radius silicon ring modulators with drive voltages of ~6 V. These compact QPSK modulators may be used in miniature optical transponders for high-capacity optical data links. © 2012 Optical Society of America

OCIS codes: 250.5300, 250.7360, 060.5060.

Silicon photonics has attracted significant attention in the last decade as a compact integration platform to implement power-efficient optical communications [1]. Silicon is a poor electro-optic material. As a result, many researchers have explored hybrid bonding of III–V materials with silicon [2] and heterogeneous epigrowth of germanium on silicon [3] to implement integrated lasers and photo detectors. However, these heterointegration devices consume similar power as those implemented in their own native nonsilicon materials. It is well known that a significant portion of the power consumption in an optical transponder comes from the electro-optic modulators and their drivers, and low-voltage silicon modulators could greatly reduce the power consumption. However, the small change of refractive index from the weak electro-optic effect in silicon poses a significant challenge to develop low-voltage silicon Mach–Zehnder interferometer (MZI) modulators, compared to those using $LiNbO_3$ and III–V semiconductors. One approach for energy-efficient silicon modulators is to use silicon microcavities. By confining light in a small area, optical intensity modulation with low drive voltages can be realized in silicon microcavities by resonant wavelength shifts. Furthermore, the much-reduced area of silicon microcavity devices, typically a few micrometers in radius, results in very small device capacitance in the order of tens of femtofarad. The reduced capacitance allows high output impedance of their electrical drivers, further lowering the power consumption.

Recently, many types of silicon microcavity modulators have been realized, such as carrier-injection silicon microring modulators [4], carrier-depletion microdisk modulators, [5] and carrier-depletion microring modulators [6]. Most of these reported microcavity modulators have focused on the on-off keying (OOK) modulation. The drive voltages can be as low as 1 V [7], and modulation speed can be as high as 30 Gb/s [8] for carrier-depletion microring modulators. Integrated on-chip heaters have been implemented to overcome narrow bandwidth challenges of microcavities [9]. These compact microring modulators can be driven by low-power flip chip bonded complementary metal oxide semiconductor (CMOS) drivers, leading to extremely low power consumption of 135 fJ/bit in the integrated transmitter [10]. Further power reduction may be demonstrated by monolithic integration of CMOS drivers with silicon photonics modulators.

Theoretical studies of quadrature phase-shift keying (QPSK) modulation using microrings have been reported in [11–13]. As seen in Fig. 1(a) and 1(b), for single-waveguide-coupled rings, the overcoupling condition (i.e., power couplings between bus waveguides and rings are larger than the round-trip loss of the rings) results in a monotonic phase change from 0 to 2π across the rings' resonant wavelengths. A proper resonance shift can generate a π-phase change while maintaining the same transmitted power at a prescribed wavelength to produce a binary PSK (BPSK) signal (a 250 Mb/s BPSK signal using microrings has been recently demonstrated in [14]). As seen in Fig. 1(c), if two BPSK ring modulators are nested in a MZI configuration, the QPSK modulation can be implemented when there is a $\pi/2$ phase difference between two arms.

We designed and fabricated a microring QPSK modulator on a silicon-on-insulator platform. Figure 1(d) shows a photograph of a fabricated device. The silicon waveguide cores have a height of 220 nm, a width of 500 nm, and a slab thickness of 90 nm. The 3 dB couplers in the MZI are multimode interference couplers. Each arm of the MZI has a microring modulator with a radius of 30 μm and a phase shifter implemented by a waveguide-based heater. As seen in Fig. 1(e), high-speed electro-optic modulation is achieved by changing the depletion width of the embedded pn junction in the core of silicon waveguide. The heater is implemented by the doped silicon waveguides, as shown in Fig. 1(f). The p and n doping levels in both pn junctions and heaters are estimated as about 5e17 cm^{-3}. Two other heaters are positioned close to the coupling regions between the rings and bus waveguides to tune the resonant wavelengths of the rings in order to compensate resonance mismatch from possible process variations. Detailed discussions on carrier-depletion microring modulators can be found in [6–7], and the junction design and fabrication of this device follows those reported in [15].

First, we measured the transmission spectra and phase response of the rings under different applied voltages.

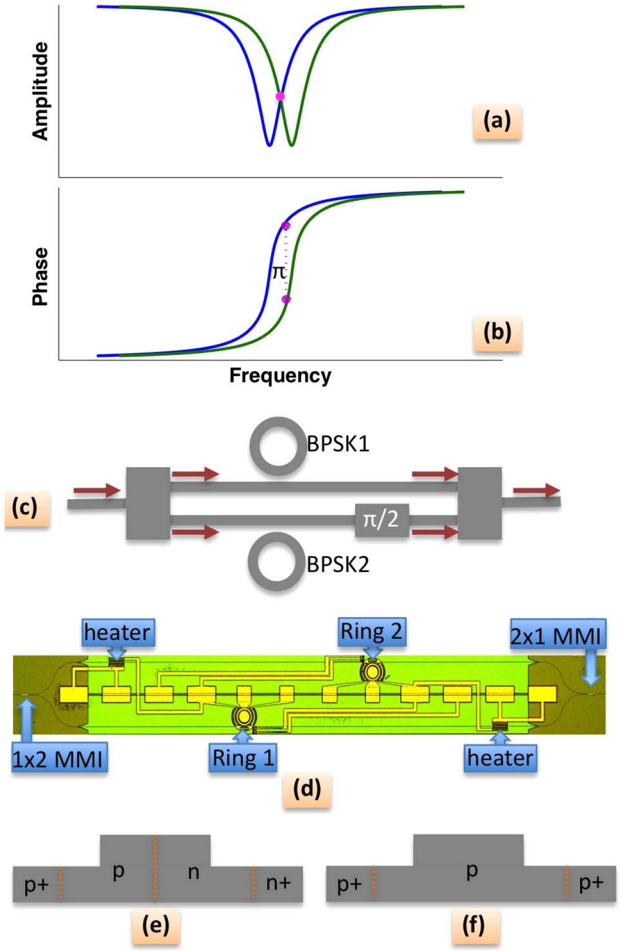

Fig. 1. (Color online) (a), (b) Transmission and phase response of a ring resonator to produce BPSK with the dotted laser wavelength at which it experiences a constant amplitude and a π-phase shift, (c) microring-based QPSK modulator, (d) microscopy optical image of a fabricated microring QPSK modulator, (e), (f) silicon waveguide cross-sections with dopings to produce high-speed modulation and thermal phase shifts.

We carried out the measurement using an optical vector analyzer based on the Jones matrix method [16]. To avoid interference effects between both rings, we set the phase difference between the two arms to zero by tuning the injection current of the heater on one of the MZI arms to maximize the output power for the off-resonant wavelengths. We also tuned the two rings to have same resonant wavelengths by controlling the heaters near the microrings. The applied reverse bias voltages on the pn junction for both rings ranged from 0 V to 6 V. The measured loaded quality factor of the rings was about 10,000, which may mainly result from the coupling between the bus and ring waveguides. The spectra in Fig. 2(a) show that the resonant wavelengths red shift with increasing reverse bias. The resonant wavelength shift per unit voltage is about 12 pm/V. The extinction ratios of the rings decrease with the increasing voltages, indicating that the overcoupling conditions are satisfied because the increasing reverse bias reduces the ring waveguide loss. The phase response of the rings is depicted under 0 V and 6 V in Fig. 2(b), demonstrating a π-phase difference for the wavelength of 1540.55 nm. The ring insertion loss at this wavelength, circled in Fig. 2(a), is approximately 7.5 dB. This insertion loss is inherent to achieve BPSK implemented by microrings. The total insertion loss would be about 10.5 dB after including an additional 3 dB loss to set the phase difference between the two arms to $\pi/2$ for QPSK modulation.

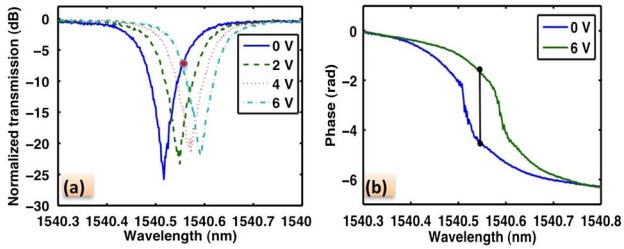

Fig. 2. (Color online) Transmission (a) and phase (b) spectra of the resonators with different bias voltages.

Next, we verify the performance of the device with 20 Gb/s QPSK modulation. To do so, a continuous-wave laser of 1540.55 nm from an external cavity laser with ~1 MHz linewidth was fed to the device. Two high-speed probes with 50 ohm terminators were applied to the two ring modulators. The driving in-phase/quadrature (I/Q) signals are inverted copies of the 10 Gb/s pseudorandom bit sequence of a length 2^{15} to –1, delayed by 32 bits from each other, and are a 6 V peak-to-peak swing with a bias voltage of 3 V. The heater currents were set to obtain a $\pi/2$ phase difference between the two MZI arms and same resonant wavelengths for the two rings. The optical output was adjusted by a variable optical attenuator and then amplified by two cascaded erbium-doped fiber amplifiers in order to achieve desired optical signal-to-noise ratios (OSNRs).

We monitored and measured the optical signal with a real-time oscilloscope with a sampling rate of 40 G/s equipped with optical coherent receivers. A homodyne detection scheme was utilized with the local oscillator power derived from the same laser source launched into the device. Offline processing of the stored real-time waveforms for both I and Q branches was used to extract the performance of modulated constellations and bit error ratio (BER). The digital signal processing (DSP) includes a digital finite impulse response filter optimized with the constant modulus algorithm and Viterbi-Viterbi feed-forward carrier recovery [17]. The BER was calculated using differential decoding and direct error counting. The recovered QPSK constellations after DSP are shown in Figs. 3(a) and 3(b) with OSNRs (0.1 nm bandwidth noise) of 30 dB and 11.5 dB, respectively, which clearly show that QPSK modulation was successfully generated using this device. Figure 3(c) depicts the measured BER versus OSNRs. At a BER of 1×10^{-3}, the required OSNR for the 20 Gb/s QPSK generated by the microring modulator was about 11.5 dB, which is approximately 3 dB higher than that of a commercial MZI QPSK modulator [18].

Both the device speed and drive voltage can be further improved by optimizing the doping levels for the pn junction. Compared with the devices in [7], the lower modulation efficiency of our device may be mainly attributed to low doping levels in the pn junction, which can be

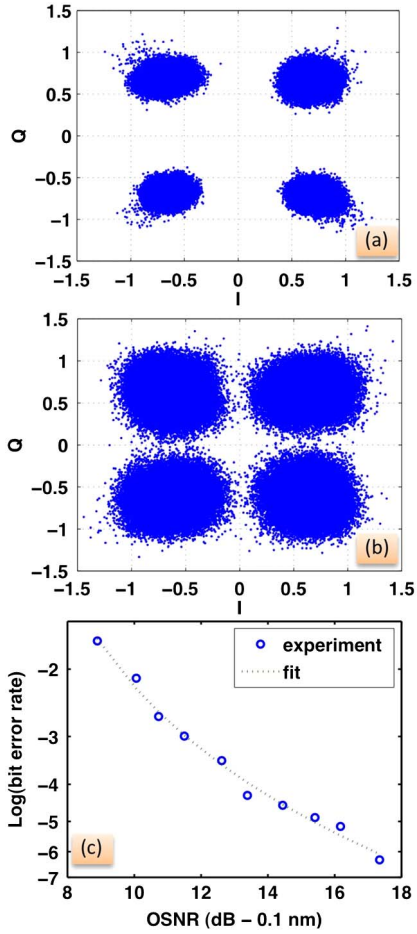

Fig. 3. (Color online) (a) I-Q constellations with an OSNR of 30 dB and (b) 11.5 dB. (c) BER performance of 20 Gb/s microring QPSK modulator.

easily fixed in the fabrication. Assuming similar resonant wavelength shift efficiency as reported in [7], a reduced drive voltage as low as 2 V is enough to produce QPSK signal. We expect that a 50 Gb/s QPSK (25 Gbaud) operation at a drive voltage of 2 V is achievable. This would promise the use of low-power CMOS drivers at a high-modulation speed. For future integrations, cascaded microring modulators on the same bus waveguide can serve as wavelength division multiplexing (WDM) over multiple wavelengths. This significantly simplifies the configuration of WDM transmitters. With its small size, more microring QPSK modulators may be integrated onto a silicon photonics platform to generate higher level modulation formats and perform many other functions for optical communications.

In conclusion, we have experimentally demonstrated the first microring QPSK modulators operating at 20 Gb/s with a peak-to-peak drive voltage of 6 V. Further improvement of the device performance can be achieved by optimizing the waveguide *pn* junctions. The ring QPSK modulators have very narrow working bandwidths, and accurately locking the ring resonance to the desired wavelengths is required to accommodate environmental temperature variations. A few preliminary studies on close-loop control of ring resonance have been reported [19], but a robust and low-power technique is yet to be demonstrated.

We thank Tsung-Yang Liow and Guo-Qiang Lo from the Institute of Microelectronics, Singapore for help in fabrication; Christopher R. Doerr, Pietro Bernasconi, and S. Chandrasekhar for helpful discussion on device characterizations; David Neilson and Martin Zirngibl for support; and Jeanette Fernandes for assistance.

References

1. R. A. Soref, IEEE J. Sel. Top. Quantum Electron. **12**, 1678 (2006).
2. A. W. Fang, H. Park, R. Jones, O. Cohen, M. J. Paniccia, and J. E. Bowers, IEEE Photon. Technol. Lett. **18**, 1143 (2006).
3. D. Ahn, C. Y. Hong, J. Liu, W. Giziewicz, M. Beals, L. C. Kimerling, J. Michel, J. Chen, and F. X. Kärtner, Opt. Express **15**, 3916 (2007).
4. Q. Xu, B. Schmidt, S. Pradhan, and M. Lipson, Nature **435**, 325 (2005).
5. M. R. Watts, D. C. Trotter, R. W. Young, and A. L. Lentine, in *Proceedings of the 5th IEEE International Conference on Group IV Photonics* (IEEE, 2008), pp. 4–6.
6. P. Dong, S. Liao, D. Feng, H. Liang, D. Zheng, R. Shafiiha, C. C. Kung, W. Qian, G. Li, X. Zheng, A. V. Krishnamoorthy, and M. Asghari, Opt. Express **17**, 22484 (2009).
7. P. Dong, S. Liao, H. Liang, W. Qian, X. Wang, R. Shafiiha, D. Feng, G. Li, X. Zheng, A. V. Krishnamoorthy, and M. Asghari, Opt. Lett. **35**, 3246 (2010).
8. J. C. Rosenberg, W. M. Green, S. Assefa, T. Barwicz, M. Yang, S. M. Shank, and Y. A. Vlasov, in *Quantum Electronics and Laser Science Conference* (Optical Society of America, 2011), paper PDPB9.
9. P. Dong, R. Shafiiha, S. Liao, H. Liang, N.-N. Feng, D. Feng, G. Li, X. Zheng, A. V. Krishnamoorthy, and M. Asghari, Opt. Express **18**, 10941 (2010).
10. X. Zheng, D. Patil, J. Lexau, F. Liu, G. Li, H. Thacker, Y. Luo, I. Shubin, J. Li, J. Yao, P. Dong, D. Feng, M. Asghari, T. Pinguet, A. Mekis, P. Amberg, M. Dayringer, J. Gainsley, H. F. Moghadam, E. Alon, K. Raj, R. Ho, J. E. Cunningham, and A. V. Krishnamoorthy, Opt. Express **19**, 5172 (2011).
11. L. Zhang, J. Y. Yang, Y. Li, R. G. Beausoleil, and A. E. Willner, in *Optical Fiber Communication Conference (OFC 2008)*, (Optical Society of America, 2008), paper OWL5.
12. W. D. Sacher and J. K. S. Poon, Opt. Lett. **34**, 3878 (2009).
13. R. A. Integlia, L. Yin, D. Ding, D. Z. Pan, D. M. Gill, and W. Jiang, Opt. Express **19**, 14892 (2011).
14. K. Padmaraju, N. Ophir, S. Manipatruni, C. B. Poitras, M. Lipson, and K. Bergman, in *CLEO: 2011–Laser Applications to Photonic Applications* (Optical Society of America 2011), paper CTuN4.
15. T. Y. Liow, K. W. Ang, Q. Fang, J. F. Song, Y. Z. Xiong, M. B. Yu, G. Q. Lo, and D. L. Kwong, IEEE J. Sel. Top. Quantum Electron. **16**, 307 (2010).
16. http://www.lunatechnologies.com/products/ova/files/OVAwhitePaper.
17. A. J. Viterbi and A. M. Viterbi, IEEE Trans. Inf. Theory **29**, 543 (1983).
18. C. R. Fludger, T. Duthel, D. van den Borne, C. Schulien, E. D. Schmidt, T. Wuth, J. Geyer, E. De Man, G.-D. Khoe, and H. de Waardt, J. Lightwave Technol. **26**, 64 (2008).
19. C. Qiu, J. Shu, Z. Li, X. Zhang, and Q. Xu, Opt. Express **19**, 5143 (2011).